Polymer Testing 145 (2025) 108764

Contents lists available at ScienceDirect

Polymer Testing

journal homepage: www.elsevier.com/locate/polytest

Experimental Investigation of the Vibration Behaviour of Variant GFRP Sandwich Panels in Thermal Environment

Philipp Hüttich *, Emil Heyden, Dieter Krause

Hamburg University of Technology (TUHH), PKT - Institute of Product Development and Mechanical Engineering Design, Denickestraße 17, Hamburg, 21073, Germany

ARTICLE INFO

Keywords:
Vibration
Experimental testing
Structural dynamics
Sandwich structure
Thermal environment

ABSTRACT

In this study, the impact of temperature on the eigenfrequencies and amplifications of four variant GFRP sandwich panels with aramid honeycomb cores is investigated. Tests are carried out at temperatures from −40 °C to 120 °C, which are typical test conditions in the aerospace industry. The tests revealed that the eigenfrequencies of these panels are highly sensitive to temperature changes, with significant changes in vibration behaviour especially noted at temperatures below 0 °C. Furthermore, the study shows that not all resonances develop most at room temperature. The specific dynamic properties and resulting resonances of the individual plates only develop under conditions of changing temperature. This finding is crucial for certification in aerospace and optimising structural design, ensuring robust performance across different operating conditions while leveraging the lightweight potential of the materials. The results highlight the complex interaction between temperature and dynamic behaviour in aerospace materials, providing essential data and insights for designing, analysing, and optimising lightweight aerospace structures. The aim of this publication is to provide initial investigations into the mechanisms behind the temperature-dependent dynamic responses in order to improve the prediction of larger structural components. This can be used in future developments to improve the safety, reliability and efficiency of aerospace systems.

1. Introduction

Due to their specific properties and high stiffness-to-weight ratio, sandwich structures are frequently used for various structural applications and have become significant in aerospace engineering, both in the primary and secondary structure of aircraft [1]. Here, GFRP sandwich panels with an aramid honeycomb core have proven to be a universally applicable material for aerospace components, as they exhibit high bending stiffness and durability [2]. However, the interaction between temperature and mechanical behaviour can significantly affect the structural integrity of sandwich panels under operating conditions [3]. Due to a lack of knowledge about the dynamic behaviour of structural components with sandwich design under temperature fluctuations, the current safety factors are often chosen conservatively, which leads to squandered lightweight potential. Vibration testing for large components at changing temperatures is hardly economically feasible from a physical point of view [4], which is why alternatives to temperature-dependent material parameter determination must be developed for the digital calculation of these large structures [5,6]. In order to ensure the reliability and safety of aerospace structures, it is essential to understand how these materials react to different environmental conditions [7]. Fibre-reinforced composites with a sandwich structure have a particularly high-temperature sensitivity that has not been adequately investigated yet. The structure of the composites with their individual layers, but also the external influences and their rates of change have a critical impact on the behaviour [8]. Their consideration in material selection, design and analysis is essential to ensure that the structures function reliably and efficiently under the operating conditions [9], emphasising the temperature-induced shift in natural frequencies. Understanding the correlation between temperature and vibration effects on structural resonances helps to optimise safety factors without compromising structural reliability. There are standardised specifications for the implementation of vibration analyses under the influence of temperature [10,11], the literature reviewed in the following suggests that, on the one hand, only a few experiments have been carried out and, on the other hand, individual test setups are used for previous studies that are suitable for the respective application [12–14]. Presumably the effort required to realise an appropriate experimental setup leads to a small amount of research data. For a homogeneous temperature distribution, a closed heating chamber with appropriate dimensions is required. This thermal chamber increases the

* Corresponding author.
E-mail address: philipp.huettich@tuhh.de (P. Hüttich).

https://doi.org/10.1016/j.polymertesting.2025.108764
Received 9 December 2024; Received in revised form 21 January 2025; Accepted 9 March 2025
Available online 17 March 2025

complexity of the test setup, as all sensors and other elements must be installed inside the chamber and designed for the corresponding test conditions, while at the same time, additional components are required for the chamber itself and its mounting in order to not influence the direct correlation between excitation and vibration response. When developing such a test rig, it is important to consider how the temperature input is to be realised. Differences in material behaviour due to an inhomogeneous temperature distribution, possibly with very high-temperature differences within a component, should be avoided.

Research has been conducted on the effects of temperature on the dynamic behaviour of sandwich structures in aviation, but due to the large variance of composite structures, there is a particular need for further investigations into valid experimental data, which are essential for material parameter identification [15–20]. Bai et al. [21,22] investigated the temperature effects on the modal properties of a sandwich structure made of carbon fibre fabric and a Nomex honeycomb core through experiments and simulations. The results show that the natural frequencies and modal damping ratios of the structure change significantly with increasing temperature, with each mode exhibiting a distinct trend. Their temperature-dependent material properties of the surface layer are identified as a major factor in the changes in mode position [21].

Numerous papers investigate the behaviour of composite structures without a sandwich core. Chandra et al. [23] investigate the dynamic behaviour of carbon fibre epoxy composite panels under different temperatures. Experimental investigations are carried out at temperatures ranging from 0 °C to 125 °C to determine the temperature-dependent elastic and damping parameters [23]. The study uses a genetic algorithm-based method to identify the parameters from modal data. It shows that the shear modulus, as the dominant elastic parameter, decreases significantly with increasing temperature [23]. Most studies investigate the influence of temperature on dynamic behaviour without experimental data, instead using simulative and analytical approaches and calculation methods [24–26]. They get comparable results, whereas the need for reliable test data is repeatedly mentioned. They all agree that temperature-dependent material properties play a significant role in the variation of material parameters, while thermal stresses only have a minor influence on the structural characteristics [26–29]. The available literature on forced vibration analysis of laminated composites under thermal conditions is limited. A detailed literature review by Garg et al. shows that in most cases shear deformation theories were used for the analysis and that all higher-order terms must be included to obtain realistic behaviour [30]. Changes in thermal and hygrothermal conditions affect the behaviour of laminates, especially for thin laminated composite panels and shell structures, with popular calculation approaches overestimating frequencies compared to layer theories and 3D solutions providing more accurate results [30].

It is striking that existing literature mainly examines the positive temperature range, although the negative temperature range also has a decisive influence on the safe use of aircraft. This study therefore investigates the resonance behaviour of typical aerospace GFRP sandwich panels with an aramid honeycomb core over the temperature range from −40 °C to 120 °C. The primary research question is how the resonance behaviour of sandwich panels changes under temperature-combined vibration test conditions. Answering this question is of crucial importance in order to be able to estimate, with the help of parameter identification and FEM calculations, whether shifts in the natural frequencies of product-related structural components can be significant enough to shift resonances even into critical frequency ranges. This represents a gap in the current practice of structural testing, in which correlations between vibration and temperature are generally not taken into account. To achieve this goal, this study fundamentally determines the material behaviour of four variant sandwich panels by experimenting on geometrically simple specimens that differ in the number of surface layers and core thickness. This investigation enhances the understanding of the fundamental reaction of GFRP sandwich elements to temperature fluctuations, expands the available database with experimental test data and creates the prerequisites for investigating entire structural components.

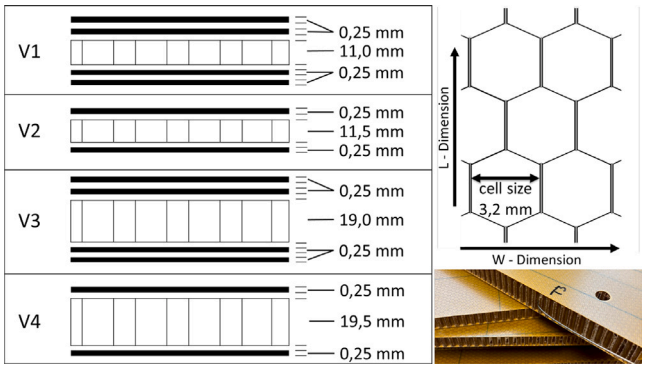

Fig. 1. Left: Structure of the four different panel types, right: honeycomb structure.

2. Materials and methods

The used GFRP sandwich panels with an aramid honeycomb core and their properties are described in detail. Afterwards, the setup of the test rig with an electrodynamic shaker, a thermal chamber and measurement technology for carrying out temperature-combined vibration tests is presented and the test setup is discussed. This information forms the basis for analysing the dynamic behaviour of the panels under various conditions.

2.1. Structure under test

The sandwich panels used were manufactured by EUROCOMPOSITES® S.A. (Echternach, Luxembourg), and are primarily used in the aerospace industry. Due to their weight-specific properties, they offer key advantages in terms of stiffness, weight and durability, even under extreme conditions. The four types of sandwiches used in this study have an aramid honeycomb core and one or two surface layers. These glass fibre-reinforced polymer facings were manufactured from AIRPREG PY 8137 using Style 7781 E-Glass as the fibre and modified phenol-formaldehyde resin as the matrix. The material properties for room temperature, according to the manufacturer, may vary, as the specific material properties depend on the sandwich structure and the manufacturing process, which can be caused, among other things, by non-uniform cooling rates and thus varying material parameters such as E-modulus [31]. According to the datasheet, the panels have a glass transition temperature of approx. 190 °C, there is no information on a lower limit temperature. Two panels have a thickness of 12 mm, with the surface layers each being 0.25 mm thick. This results in a core thickness of 11 mm for the panel with two surface layers on each side (Variant V1) and a thickness of 11.5 mm for the panel with one surface layer on each side (Variant V2). The other two panels have a thickness of 20 mm, with the surface layers also being 0.25 mm thick. This results in a core thickness of 19 mm for the panel with two surface layers on each side (Variant V3) and a thickness of 19.5 mm for the panel with one surface layer on each side(Variant V4). An exemplary representation and the layer structure are shown in Fig. 1.

2.2. Test setup

Electrodynamic shakers are widely used and are available in various sizes and with different force ranges [32–34]. They are capable of generating different types of signals and a range of frequencies. The working principle is suitable for medium- to high-frequency investigations, but with certain limitations due to the displacement range in the low-frequency range [35,36]. The electrodynamic shaker used (SD5208, Spectral Dynamics, San Jose, USA) has a force vector of 24 kN, so there is sufficient power reserve for the dynamic investigations. In order to achieve reproducibility, accuracy and consistency of

Fig. 2. The environmental chamber at the electrodynamic shaker.

the temperature field, a flow-optimised test chamber tailored to the shaker was developed. Fig. 2 shows the combined test environment, consisting of the electrodynamic shaker and the thermal chamber. This chamber is mounted above the shaker and mechanically decoupled from the vibrations. The air temperature is controlled by an air conditioning unit (TempEvent, Weiss Technik GmbH, Reiskirchen, Germany), which supplies temperatures between −55 °C and 150 °C at a maximum volume flow of 300 m^3/h. To protect the slip table of the shaker from extreme temperatures, a thermal barrier made of glass fibre hard fabric, which has almost no damping or temperature-dependent properties, is fitted under the sample.

For vibration excitation, the sample was clamped from both sides, each with a flange fixed by a screwed connection. The flanges are connected to the slip table of the shaker via screw connections. Although this clamping has disadvantages compared to a mechanical decoupling from the environment, such as in Chandra et al. [23], it is a very robust and repeatable way to examine larger or heavier test specimens and is frequently used in experimental and simulative investigations [21,37]. In order to ensure a defined load application and to prevent any influence from the flanges even at high temperatures, they are designed to be as rigid as possible and made of hardened stainless steel so that temperature-related changes in material properties can be assumed to be negligible. To avoid mechanical damage to the sandwich structure during clamping and to minimise surface pressure and stress peaks while generating a high number of eigenmodes, the panels with a size of 400 mm × 197 mm were clamped eccentrically on an area of 50 mm × 50 mm with a defined torque of 15 N m at a uniform surface pressure. The resulting compressive stress is below the maximum compressive load specified in the datasheet. Accelerometers of the type PCB-TLD356A02 and PCB-339B31/NC (PCB Piezotronics Inc., Depew NY, USA) were used to measure the acceleration behaviour of the panels. The accelerometers have a measuring range of 1 to 5000 Hz and a resolution of 0.005 m/s^2. These sensors were attached to the flange and two corners of the sample. The acceleration sensor on the flange is used to normalise the acceleration of the sample when evaluating the tests with the acceleration of the sensors of the slip table. By using two sensors at different points on the sample, it is possible to ensure that all eigenmodes are recognised. This is necessary because eigenmodes develop to different degrees at certain points and may not be visible in the frequency response function (FRF). Before clamping in the test rig, the acceleration sensors were glued to the sample. To ensure that the position of the sensors is the same for all samples, the sensors were positioned using a template and attached at a distance of 5 mm from the edges as shown on the right in Fig. 3.

The temperature is measured at different points on the specimen and in the thermal chamber to ensure that the desired test temperature is reached at all points on the specimen during the tests. Thermocouple type K temperature sensors (ThermoExpert GmbH, Stapelfeld, Germany) were used for this purpose and measured at the top, centre and bottom of the chamber, and also measured at the top, centre and bottom of the sample. In addition, a temperature sensor was inserted into the honeycomb structure of the panel to ensure that the temperature was not only measured on the surface but also inside the specimen. This way, the temperature gradient across the sample can be determined in the evaluation. Fig. 3 shows the experimental setup inside the temperature chamber and the arrangement of the sensors. Data from all sensors are processed using the HBM QuantumX system (MX840B and MX1601, Hottinger Brüel und Kjaer GmbH, Darmstadt, Germany). The signals are recorded with NI Diadem 2019 (National Instruments Corp., Austin, USA) at 9600 Hz and analysed in Matlab 2022b (The MathWorks Inc., California, USA). The selected sample rate ensures that the sinusoidal oscillation can also be approximated in the upper-frequency range during the Fast-Fourier-Transform (FFT). The resulting amplification HI is the ratio of the Fourier-transformed signal from the sensor on the sandwich plate to the peak amplitude of the input signal (see Eq. (1)). This allows the dynamic behaviour of structural components to be investigated under different load conditions and their resonance frequencies and damping properties to be characterised.

$$HI_{out,in} = \frac{a_{out}}{a_{in}} \tag{1}$$

The excitation of the slip table attached to the shaker is vertical to the mounted panels, while the shaker generates a controlled vibration. The gain and frequency of the vibrations are controlled using VibrationVIEW control software (Vibration Research, Jenison, USA) and a 50 g accelerometer PCB-352C33 (PCB Piezotronics Inc., Depew NY, USA) mounted on the slip table to simulate specific test conditions. To minimise the time required for the experiments, the specimens were excited with a logarithmic sine sweep at 2 oct/min. The sweep was performed starting from 10 Hz to 600 Hz and following back from 600 Hz to 10 Hz. The temperature was changed in steps of 20 °C, resulting in nine temperature levels. A total of 72 tests were therefore carried out. A total of six sweeps per panel were performed at each

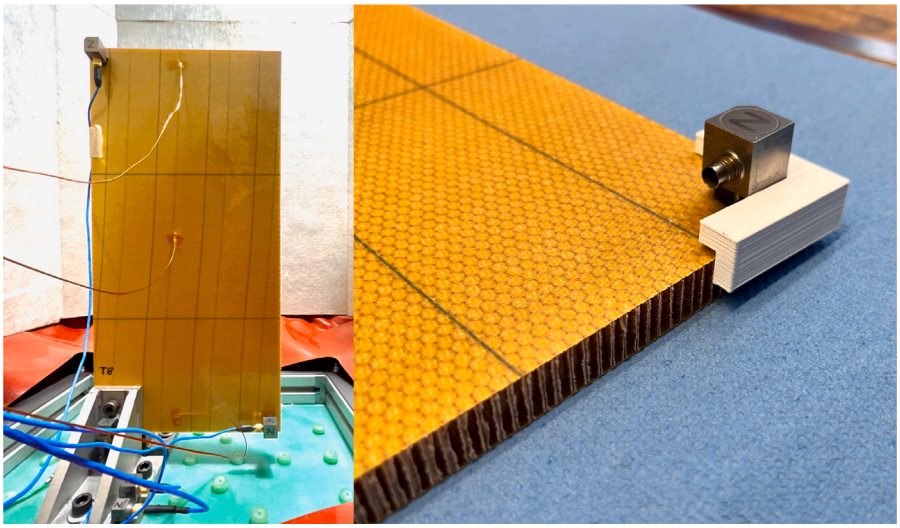

Fig. 3. Left: Panel mounted in the Chamber with acceleration and temperature sensors, right: positioning of the acceleration sensors.

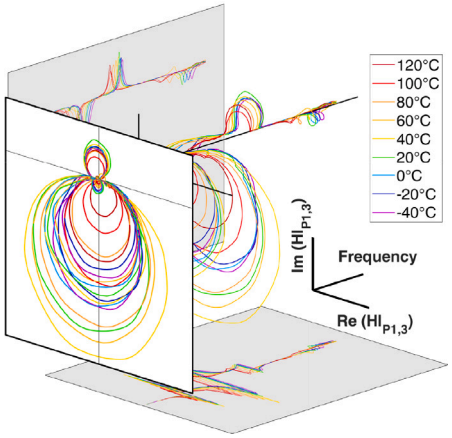

Fig. 4. Locus curve of 12 mm panel with two surface layers (V2) at point P3.

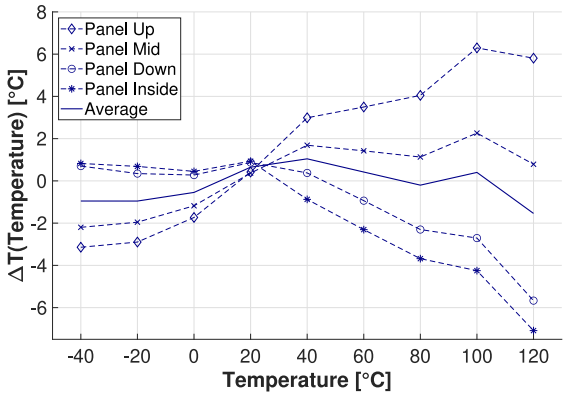

Fig. 5. Nominal temperature gradient of the test specimens.

temperature level, three upsweeps and three downsweeps. Minor non-linearities between upsweep and downsweep were normalised. With two test specimens of each type investigated, the average was formed from 12 FRFs at each level between −40 °C and 120 °C for statistical validation. The respective frequency response functions of the tests for all panels and temperatures are published as raw data [38]. As the standard deviation in the frequency ranges between the resonances was negligible, the standard deviation of the individual resonances is shown in Fig. 11. Preliminary tests showed that the sandwich panels exhibit non-linearities even at low deflections as a result of the mode-specific deformation, which became particularly clear when comparing the upsweep and downsweep signals and was reflected in an asymmetry of the phase-specific locus curve. For this reason, the acceleration was set to a constant peak acceleration $a_{in} = 2$ m/s^2 as a compromise between the lowest possible excitation acceleration of the shaker and the most linear vibration behaviour of the sandwich panels. Fig. 4 shows an example of the temperature-dependent frequency response of the 12 mm panel with two surface layers at point P3 as a locus curve during an upsweep with an acceleration of 2 m/s^2. It can be noted that the panel exhibits almost symmetrical behaviour, i.e. the panel retains comparatively linear properties despite deflection.

3. Test results and discussion

Overall, the frequency response functions of the identical specimens at the same temperature conditions differed only very slightly from each other with a maximum deviation of 3.29 °C. Fig. 5 shows the average temperature deviation of all panels as a function of the sensor position over the nominal temperature. Despite the flow optimisation, temperature gradients in the climate chamber and consequently in the sandwich panel cannot be completely avoided. The temperature deviates most strongly in the upper part and inside the panel, whereas the panel thickness only has a minor influence on the temperature difference. The deviations are approximately proportional to the temperature gradient to room temperature and therefore show a greater deviation of a maximum of 6 °C in the high temperature range at 100–120 °C, while a maximum deviation of −3 °C is recorded in the low temperature range at −40 °C. The average temperature of all sensors is almost constant and only deviates between 1.0 °C and −1.5 °C from the nominal temperature. No delamination or other optically recognisable changes to the structure occurred in the temperature range tested.

To get an impression of the resonance changes, the resonance behaviour of the 12 mm panel with two surface layers is discussed qualitatively as an interpolated spectrogram. Fig. 6 shows the resonance and amplitude changes of the panel as a function of temperature. The red lines of data points visualise FRFs generated at each of the nine

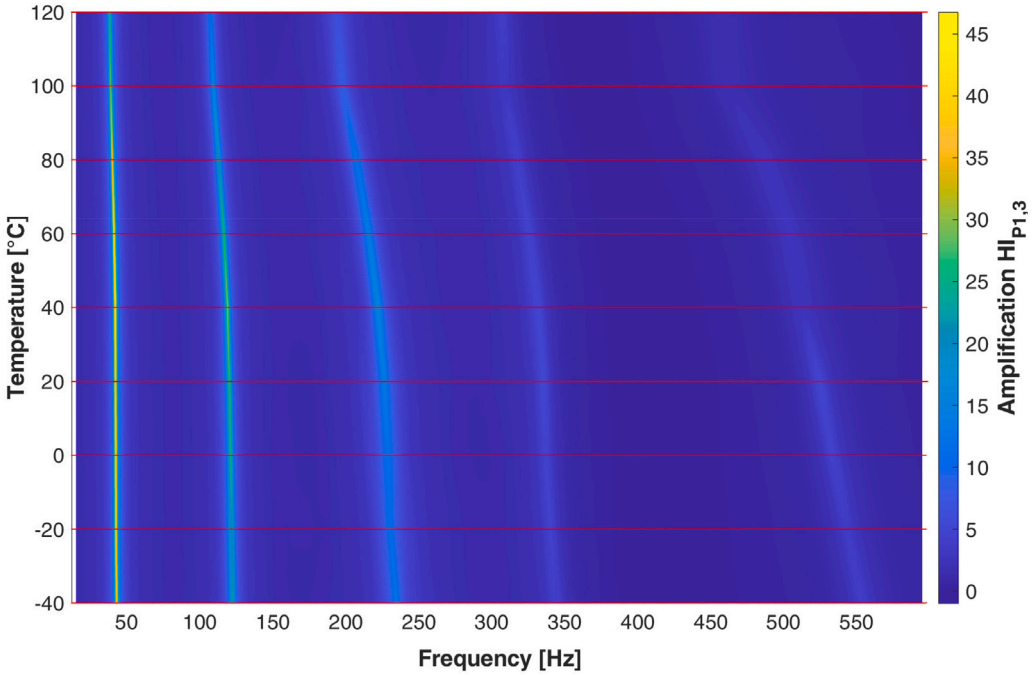

Fig. 6. FFT-based interpolation of temperature depended frequency-shift of type V2.

temperature levels in an upsweep. The temperature between the nine FRFs is interpolated by a surface, resulting in the spectrogram of the amplification as a function of frequency and temperature. It is obvious that the temperature has a significant influence on the eigenmodes and the amplification of the panel. In general, it can be said that the damping and associated amplification of the vibration behaviour is strongly temperature-dependent, especially in the low-frequency range. As in the previously mentioned literature, the amplification decreases with increasing temperature due to proportional damping effects, but the results also show that the vibration behaviour is damped at colder temperatures. The resonance frequencies clearly shift with increasing temperature, whereas it becomes apparent that the modes have different frequency shift gradients and the shifts increase with higher temperature. The non-linear behaviour of the modes over temperature can be seen at all resonances, but particularly at the third and fifth resonance. Between –20 °C and 40 °C the modes shift almost linearly, from 40 °C the gradient increases and is at its maximum between 60 °C and 100 °C. From 100 °C to 120 °C the shift decreases again. A striking aspect is the temperature range between –40 °C and –20 °C, which has been considered very rarely in the literature, but is crucial for aviation. The gradient increases here too, which leads to an increased shift in the modes.

The frequency response functions and phase diagrams at both measuring points P3 at the upper end of the panel and P2 in the lower corner of the panel are also analysed. This is shown for the four variants in Figs. 7–10, the resonance frequencies with respective amplification at the measuring point P3 are listed in Tables 1–4. In the following section, the characteristics of functions as well as the similarities and differences between the panels are discussed. It should be noted that only the mean values of the upsweeps are shown below. The thick-core panels have four eigenmodes in the analysed frequency range, while the thin-core panels have five eigenmodes. A temperature-induced shift in the resonances can be clearly recognised in all four panels. This shift is mode-dependent and generally increases with increasing frequency. While the first eigenmode is particularly prominent for the upper measuring point, the maximum amplification occurs at the third eigenmode for the lower measuring point. The amplification also shows a strong temperature dependence for all four variants. In general, a reduction in amplification can be measured at higher and lower temperatures. However, the maximum amplification does not always occur at a temperature of 20 °C, which is commonly used for resonance testing of structural components without combined test conditions.

The natural frequencies of variant V1 shift between 6.3 Hz at the first resonance, which corresponds to 12.9%, and 122 Hz at the highest resonance in the analysed frequency range, i.e. 21.1%. The natural frequencies in a higher frequency range shift significantly more than in a lower frequency range. The natural frequencies drift more strongly when the temperature shifts into the positive than into the negative range. Between 40 and 120 °C, the natural frequencies shift by an average of 32.4 Hz or 11.4%. Between 40 °C and −40 °C, the natural frequencies shift by an average of only 17.3 Hz or 5.7%.

One important finding is that the characteristics of the resonances are temperature-dependent, but the individual resonances react differently to the individual temperatures. In contrast to the generally valid test temperature of 20 °C, the panel has an increased resonance behaviour at deviating temperatures. As it can be seen in Table 1 and Fig. 7, the first mode shows its maximum resonance at 0 °C, the second mode at 20 °C and the third mode at −40 °C. Temperature changes have a direct impact on the damping factor. In many systems, especially in the materials analysed here, the temperature influences the internal damping. Both higher and lower temperatures increase the attenuation by changing the material properties. As a result, the phase shift curves in the resonances show a changed transition. The curves in the phase diagrams illustrate how the phase shift behaves over a wide frequency range for different temperatures. At lower temperatures, sharper and more prominent phase changes occur, while at higher temperatures the phase changes are flattened. This indicates that the material is more damped at higher temperatures, which reduces the amplitudes of the oscillations and smoothes the phase shifts. At higher temperatures, clear changes in the phase shift can be recognised, particularly in higher frequency ranges due to a changed phase response. This indicates that the material or system responds differently at these temperatures than at lower temperatures. The phase curves tend to be less prominent, which indicates that the system is more damped at these temperatures and the damping behaviour is clearly evident. This panel also demonstrates significant effects in terms of damping influences and altered vibration behaviour in the phase diagram. This behaviour, which occurs particularly at higher temperatures, in turn, provides information about

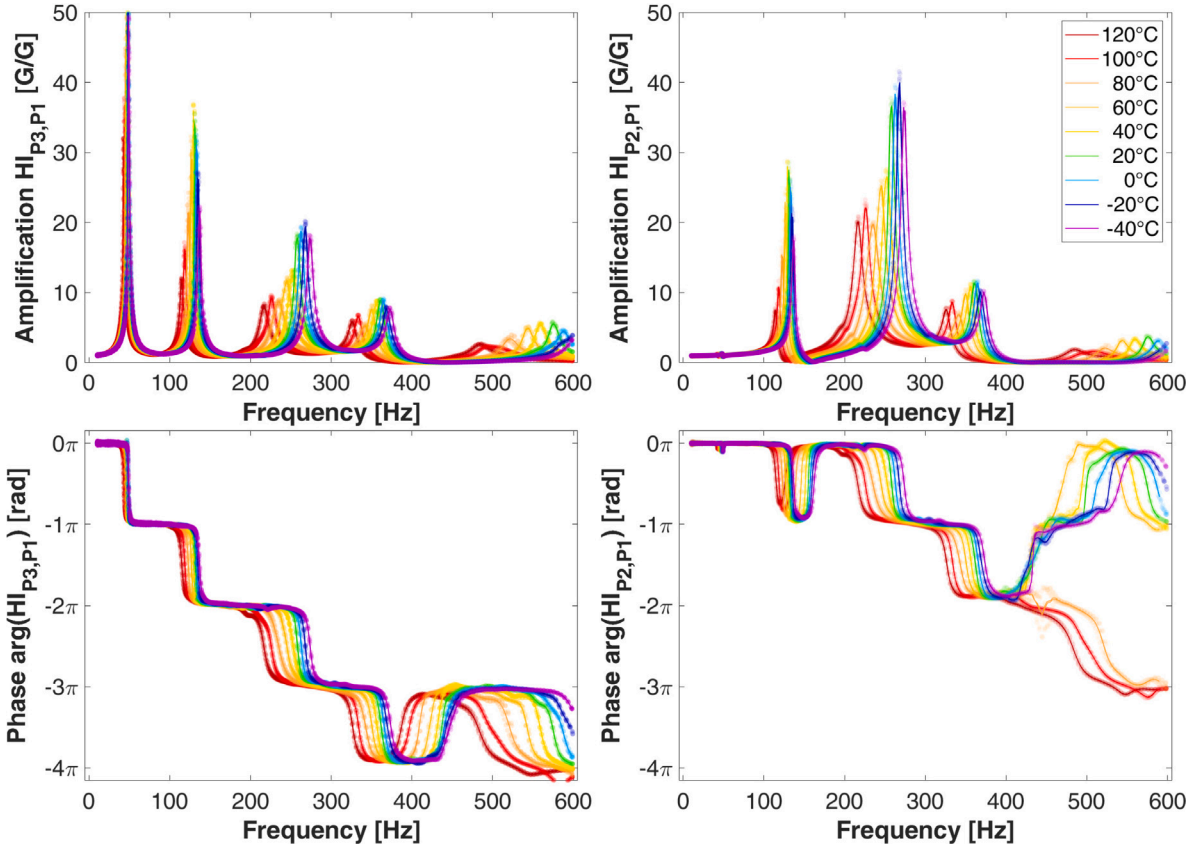

Fig. 7. Temperature-dependent FRF and phase diagrams for 12 mm panels with two surface layers (V1).

Table 1
Temperature-dependent mode changes with the specific amplifications at P3 for 12 mm panels with two surface layer (V1).

Temperature [°C]	1. Mode		2. Mode		3. Mode		4. Mode		5. Mode	
	f [Hz]	HI	f [Hz]	HI	f [Hz]	HI	f [Hz]	HI	f [Hz]	HI
120	43.40	31.36	116.90	11.17	219.00	8.45	328.70	5.55	490.10	3.24
100	44.50	35.22	119.90	14.88	228.10	10.46	334.90	6.76	506.70	3.41
80	45.80	41.89	125.00	21.65	239.80	10.79	344.40	7.57	524.80	3.60
60	47.00	47.04	128.90	25.38	249.30	10.13	352.50	7.82	545.70	3.18
40	47.90	50.56	131.60	31.32	257.80	12.70	357.10	8.61	568.90	3.73
20	48.30	49.05	134.00	32.71	260.80	14.17	363.60	8.59	575.20	5.12
0	48.90	50.70	134.90	30.34	264.40	14.79	365.80	7.73	586.70	4.73
−20	49.40	49.36	136.90	26.47	270.40	14.67	368.80	6.73	600.30	4.13
−40	49.70	47.61	138.80	24.08	276.00	14.94	373.70	7.05	612.90	4.18

the characteristics of the individual resonances. Like variant V1, variant V2 with only one surface layer has five natural frequencies in the analysed frequency range. The natural frequencies are all below the equivalent modes of V1, which can be explained by only one surface layer and the associated lower stiffness. The natural frequencies of variant V2 shift between 4.8 Hz and 93.5 Hz, although the shifts are smaller than for variant V1 with two surface layers. The fifth natural frequency shifts the most by 16.90%. In principle, the displacement also increases for variant V2 at higher natural frequencies. It can also be observed with this variant that the natural frequencies shift more in the positive direction than in the negative direction. Between 40 °C and 120 °C, the natural frequencies shift by an average of 25.65 Hz or 10.13%. Between 40 °C and −40 °C, the natural frequencies shift by an average of only 14.94 Hz or 5%. This variant shows the maximum amplification for the first three resonances at 40 °C

With the 20 mm panels, only four resonances occur in the analysed frequency range. Due to the geometric shape and rigidity of the panel in connection with the mounting, an anti-resonance occurs at the second resonance, which is shown both in the frequency response function and in the phase diagram in Fig. 10. Due to the comparability to the other variants, the clamping surface, with which this effect could be eliminated, was not changed, but must be taken into account accordingly in the analysis.

The natural frequencies of variant V3 shift between 8.7 Hz and 81.4 Hz. The first natural frequency also shifts the least at 8.6 Hz or 10.3% and the fourth natural frequency shifts the most at 81.4 Hz or 11.6%. With variant V3, the natural frequencies also shift more in the positive direction than in the negative direction. The average shift from 40 to 120 °C for variant is 27.3 Hz or 9.93%. In contrast, the average shift from 40 to −40 °C is only 14.34 Hz or 5.14%. The shift is correspondingly lower than for the 12 mm panel with two surface layers. This suggests that the core has a lower temperature sensitivity than the cover layers. In comparison to the thin variants V1 and V2, the phase change is stable and does not change depending on the temperature, but here too the flattening of the phase curve shows sandwich-internal damping processes.

The shift due to the temperature is also pronounced to a different level for each natural frequency in variant V4. Table 4 shows that the

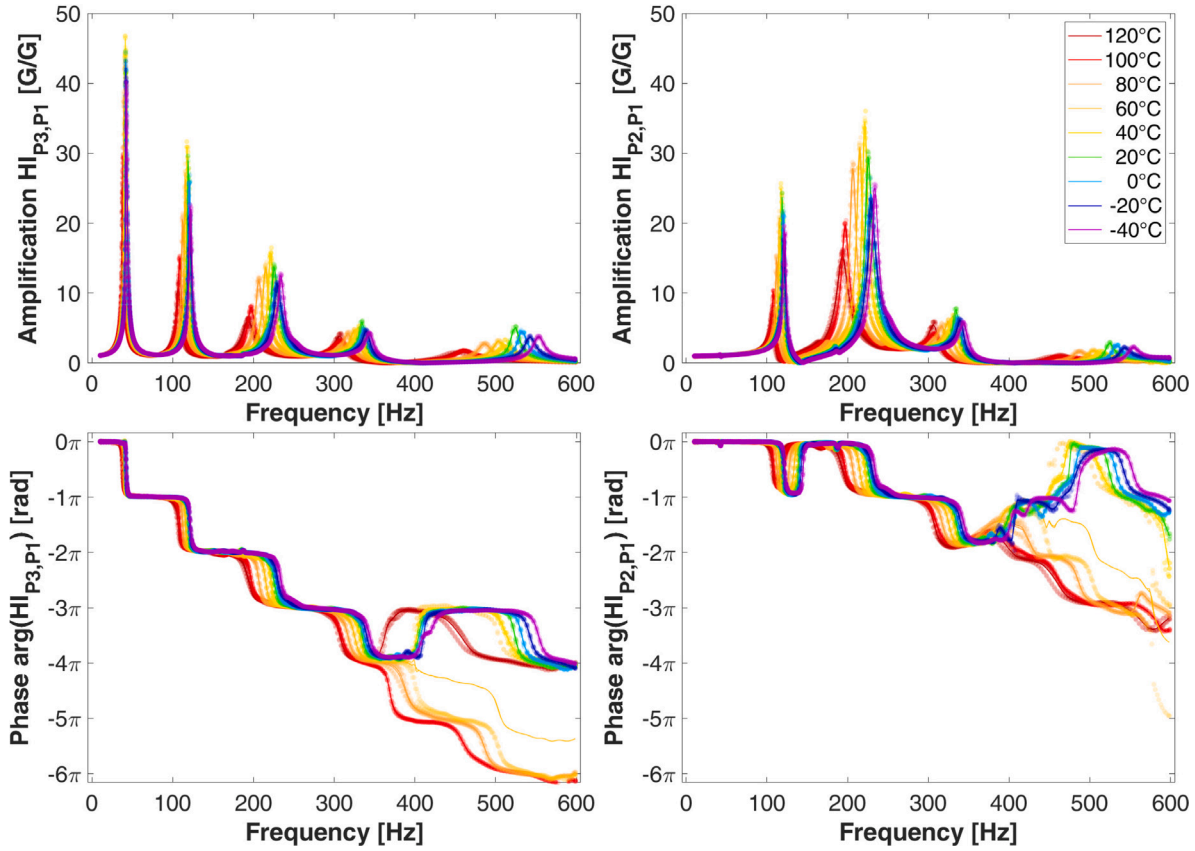

Fig. 8. Temperature-dependent FRF and phase diagrams for 12 mm panels with one surface layer (V2).

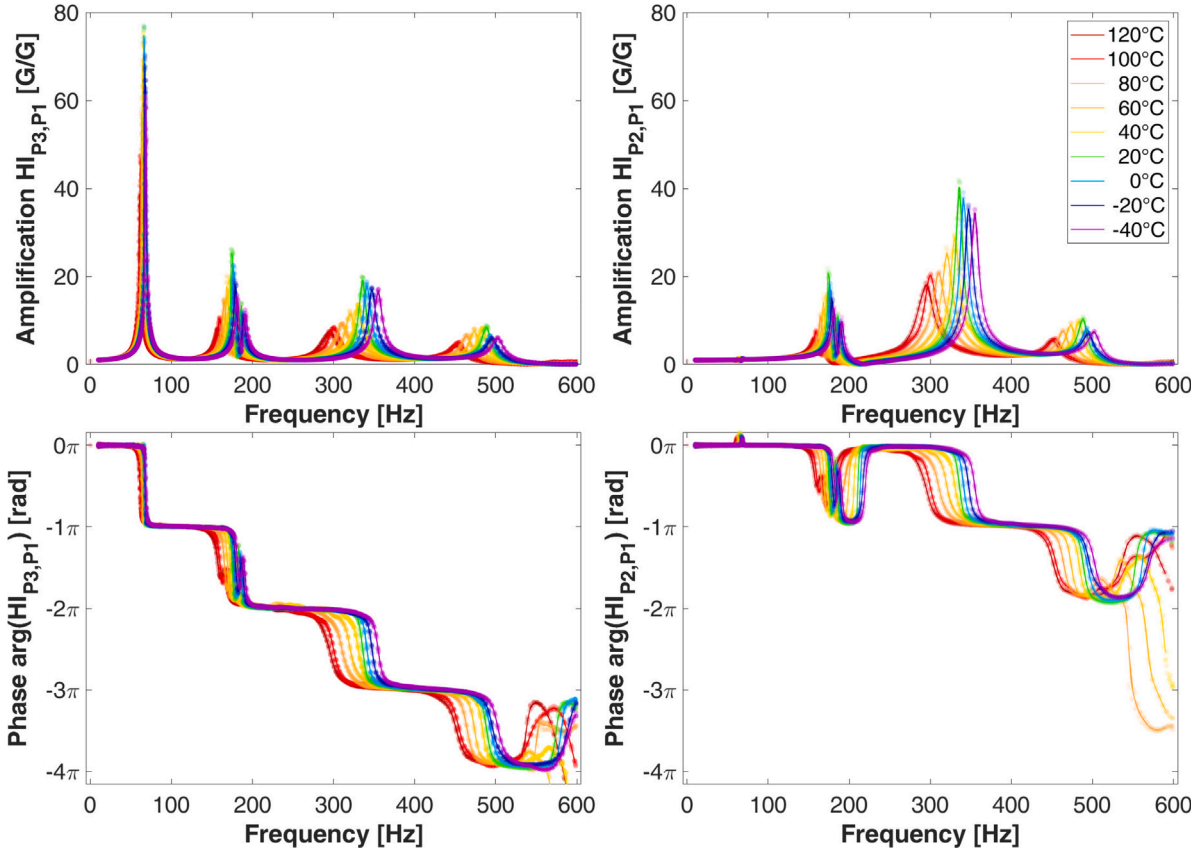

Fig. 9. Temperature-dependent FRF and phase diagrams for 20 mm panels with two surface layer (V3).

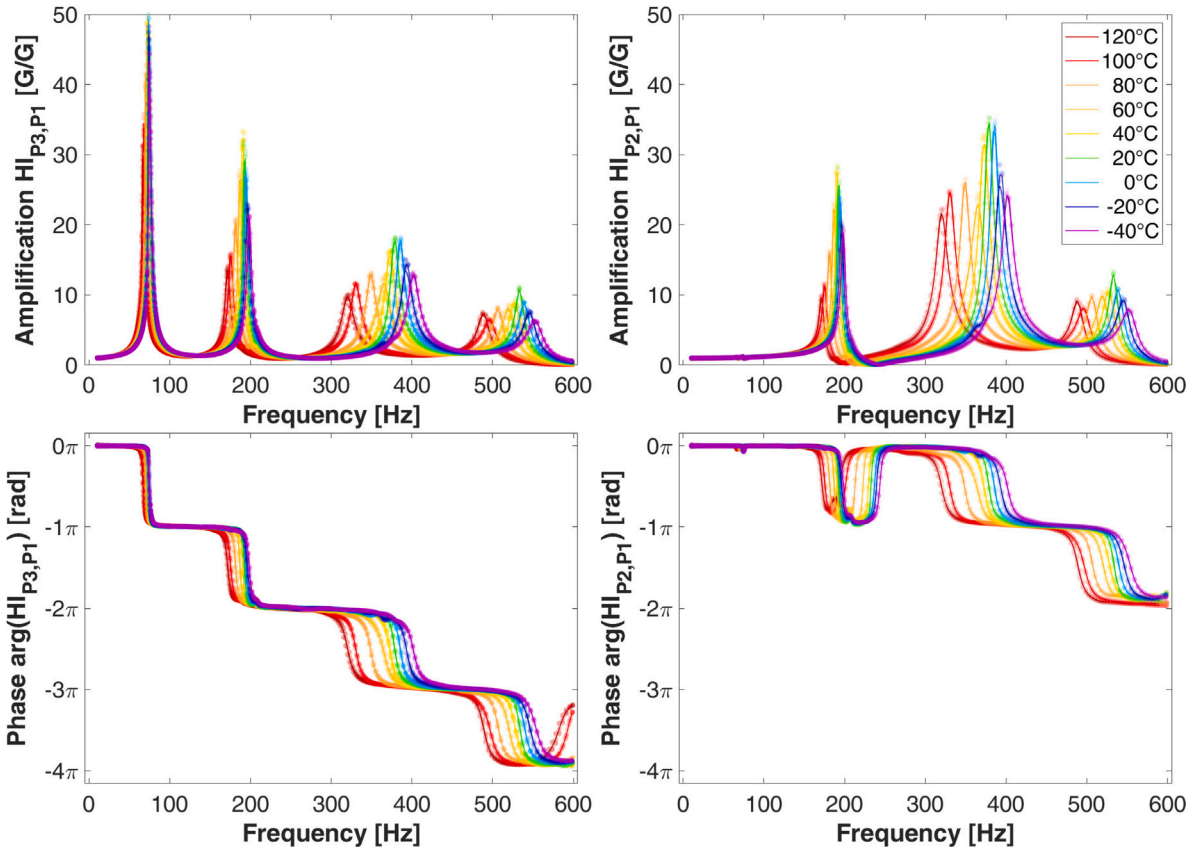

Fig. 10. Temperature-dependent FRF and phase diagrams for 20 mm panels with one surface layer (V4).

Table 2
Temperature-dependent mode changes with the specific amplifications at P3 for 12 mm panels with one surface layer (V2).

Temperature [°C]	1. Mode		2. Mode		3. Mode		4. Mode		5. Mode	
	f [Hz]	HI	f [Hz]	HI	f [Hz]	HI	f [Hz]	HI	f [Hz]	HI
120	38.10	24.53	107.30	10.71	193.80	6.17	306.50	3.86	460.20	1.60
100	38.70	29.00	108.90	15.00	196.90	8.01	308.50	3.24	460.30	1.79
80	39.90	36.52	112.70	20.34	206.60	11.84	316.90	4.20	486.50	2.77
60	41.10	41.44	116.30	26.26	215.20	13.73	325.10	4.65	503.40	3.09
40	41.90	43.75	118.70	29.55	222.20	15.43	331.60	5.01	512.20	2.59
20	42.00	39.90	119.90	27.09	226.10	13.67	334.60	5.64	524.60	5.13
0	42.30	40.47	121.00	25.79	228.70	11.46	336.10	4.64	531.60	4.38
−20	42.40	39.78	121.80	20.75	230.10	11.19	340.20	4.63	542.40	3.78
−40	42.90	38.39	122.60	21.96	233.80	12.09	343.30	4.21	553.90	3.78

Table 3
Temperature-dependent mode changes with the specific amplifications at P3 for 20 mm panels with two surface layer (V3).

Temperature [°C]	1. Mode		2. Mode		3. Mode		4. Mode	
	f [Hz]	HI	f [Hz]	HI	f [Hz]	HI	f [Hz]	HI
120	66.70	30.58	170.80	13.61	319.90	9.78	487.50	7.34
100	67.70	34.48	174.60	15.53	329.60	11.55	494.90	6.43
80	69.80	41.53	181.20	20.41	349.50	12.67	506.30	8.10
60	71.60	48.34	186.00	26.40	364.30	11.60	518.90	8.10
40	72.90	50.44	190.30	32.05	373.00	15.65	527.80	8.67
20	73.00	45.25	192.20	29.15	378.90	17.71	533.00	10.75
0	73.80	49.31	194.20	27.30	384.20	17.33	539.00	8.83
−20	73.90	47.26	196.00	20.96	392.60	13.42	546.30	7.44
−40	74.40	43.02	197.50	20.89	401.10	12.87	551.50	6.32

first eigenfrequency only shifts by 6.6 Hz, while the fourth eigenfrequency shifts by 50.2 Hz. On average, the eigenfrequencies shift over the temperature range from −40 °C to 120 °C by 30.68 Hz or 12.03%.

Fig. 11 summarises the percentage change in the frequency of the individual modes of all four sandwich variants at different temperatures. The four diagrams show the temperature dependency of

Table 4
Temperature-dependent mode changes with the specific amplifications at P3 for 20 mm panels with one surface layer (V4).

Temperature [°C]	1. Mode		2. Mode		3. Mode		4. Mode	
	f [Hz]	HI	f [Hz]	HI	f [Hz]	HI	f [Hz]	HI
120	61.20	37.35	156.70	7.66	295.90	7.37	451.00	4.30
100	62.30	45.06	160.20	10.25	300.30	8.33	454.70	4.99
80	64.00	54.51	165.80	14.17	311.00	9.23	464.00	6.57
60	64.30	69.32	168.10	17.92	320.20	11.41	472.70	7.42
40	65.40	73.64	172.10	18.68	329.90	13.42	483.90	8.05
20	66.00	74.91	174.70	25.26	335.10	19.20	488.50	8.58
0	66.50	74.21	176.40	22.05	340.60	18.22	492.80	6.44
−20	67.20	68.51	178.50	18.37	347.20	17.07	495.00	5.89
−40	67.80	61.36	180.90	15.46	354.50	16.71	501.80	6.06

the normalised frequency shift as a function of the different temperatures. A general trend of decreasing frequency with increasing temperature can be observed for all four sandwich panels, but the resonance frequency of the panels is not reduced linearly by increasing the temperature. This does not only apply to the positive temperature range, in the negative temperature range the opposite behaviour can be observed, the resonance frequencies increase. This clearly shows how the structural properties such as the rigidity of the panels can change under changing thermal environments. The five eigenmodes generally show similar trends in all diagrams, but the exact dependency of the variants differs. In a comparison of the four panels, the thinner sandwich panels show a stronger temperature dependency, while the panels with a thicker honeycomb core exhibit a more stable behaviour with regards to frequency changes when the temperature changes. This effect is particularly noticeable in the higher temperature range. The variants with two surface layers respond even stronger to temperature changes than the variants with one surface layer. This indicates that the surface layers of the panels react more sensitively to temperature changes, while increasing core thickness tends to have a stabilising effect. The graphs in Fig. 11b displays a summary of the percentage change in amplification of the individual modes of all four sandwich variants at different temperatures. In the four diagrams, the temperature dependency of the normalised amplification change is shown as a function of the different temperatures. In general, it can be observed that the amplification of the eigenfrequencies decreases towards the edge temperatures, while the loss increases. Although the amplification also increases for other variants above the normalised 100% at 20 °C, the 12 mm panel with one surface layer is striking, with the first three eigenmodes showing their maximum amplification at 40 °C, which is approx. 10% higher than at 20 °C. The materials and sandwich composites of the structures are less stable at extreme temperatures, which is reflected in increased damping and reduced amplification of the vibrations.

First of all, it can be observed for all specimens that the eigenmodes shift to lower frequency ranges as the temperature increases. This shift is not linear. At higher temperatures, the eigenfrequencies of the tested panels shift more than at lower temperatures, but the shifts in the low temperature range are by no means negligible. It could be shown that the resonances shift more in higher frequency ranges than in lower frequency ranges. The structural design also has an influence on the temperature-related shift. The investigation shows that a thicker honeycomb core reduces the temperature-related shift. This means that thicker panels are more stable and less susceptible to changes in their resonance frequencies when the temperature changes. On the other hand, more surface layers increase the temperature-induced displacement. This indicates that panels with multiple surface layers are more sensitive to temperature changes and show greater shifts in their resonance frequencies. These findings are crucial for the selection of suitable material configurations in applications where temperature stability plays an important role. It can also be seen that the damping of the system increases with temperature. At lower temperatures, especially below 0 °C, the damping is lower, which leads to stronger and sharper phase shifts. At higher temperatures, on the other hand, damping increases, resulting in smoother phase shift curves and less pronounced resonance behaviour. These observations are typical for many materials that lose structural stiffness at higher temperatures and at the same time exhibit higher internal damping. Comparable studies consistently cite temperature-dependent material properties as the main reason for the change in modal parameters [22]. This behaviour has an influence on the application of the material in environments with different temperatures, such as aerospace, as the dynamic properties, in particular the resonance frequency and damping, are strongly temperature-dependent, as shown. In summary, the variance of the four panels can be characterised as the following:

- Thicker honeycomb cores reduce temperature-induced shifting.
- Additional surface layers increase the temperature-related shift.

4. Conclusion

In this study, the influence of temperature on the eigenfrequencies and amplifications of four different GFRP sandwich panels with an aramid honeycomb core was thoroughly investigated in combined vibration tests. The results show several aspects of the dynamic behaviour of these aerospace materials over the typical aerospace temperature range of −40 °C to 120 °C. Primarily, it was shown that the eigenfrequencies of the sandwich panels are strongly sensitive to temperature changes. In particular, resonances at higher frequencies tend to lead to higher shifts due to temperature. Moreover, contrary to original expectations, significant frequency shifts were observed at temperatures below 0 °C. This highlights the need for comprehensive testing and analysis under extreme environmental conditions, in order to accurately predict the dynamic behaviour of sandwich panels in realistic operating conditions. In addition, the study shows that the amplifications are not consistently highest at room temperature, as currently assumed in aviation certification. Instead, the amplification values reach their maximum in different temperature ranges, depending on the specific properties of the sandwich panels. Understanding the temperature-dependent amplification behaviour is crucial for optimising the structural design and ensuring robust performance under different operating conditions while considering the lightweight potential. Overall, the results presented in this study highlight the inherent interactions between temperature and dynamic behaviour in aerospace sandwich panels. By experimentally investigating the temperature-induced shifts in eigenfrequencies and amplifications, this study contributes valid data and insights for the design, analysis and optimisation of lightweight structures. Further research is required to investigate the underlying mechanisms of temperature-dependent dynamic behaviour, also as a function of core thickness. The experimental

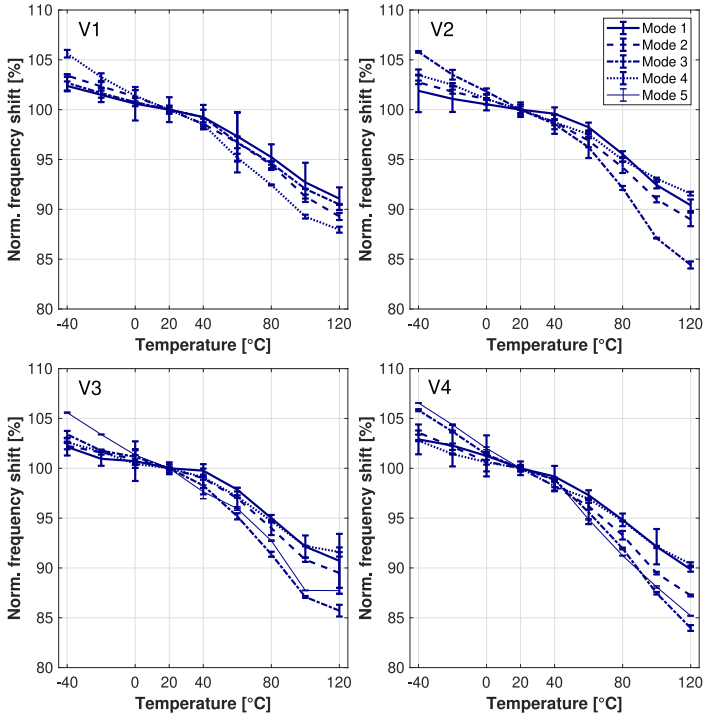

(a) Frequency-shift for the four variants

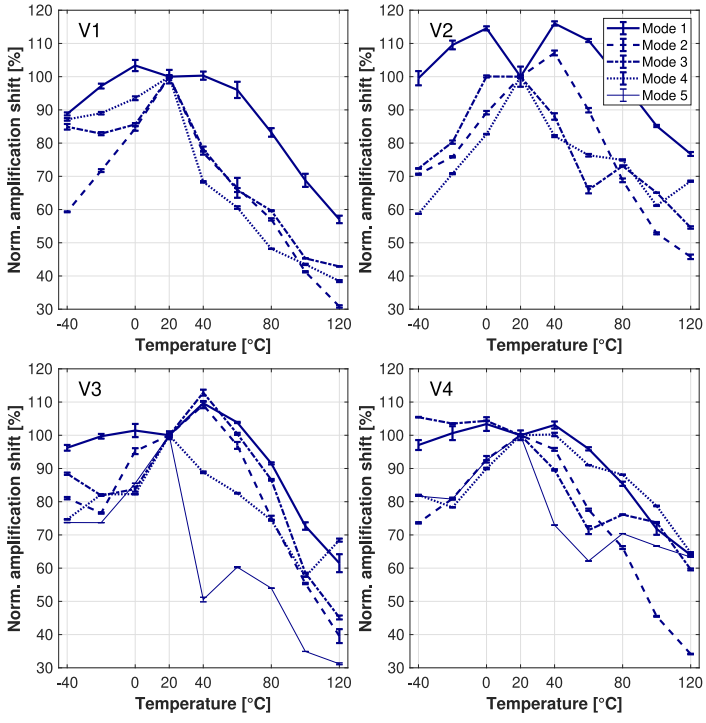

(b) Amplification-shift for the four variants

Fig. 11. Normalised shift of frequency and amplification as a function of temperature.

data can be used to develop and support numerical prediction models for a more accurate performance estimation of even large structural components. By improving the understanding of these interactions, the safety, reliability and efficiency of aerospace systems can be increased in a rapidly evolving technological landscape.

CRediT authorship contribution statement

Philipp Hüttich: Writing – review & editing, Writing – original draft, Visualization, Methodology, Investigation, Data curation, Conceptualization. **Emil Heyden:** Validation, Conceptualization. **Dieter Krause:** Project administration, Funding acquisition.

Declaration of competing interest

The authors declare that they have no known competing financial interests or personal relationships that could have appeared to influence the work reported in this paper.

Acknowledgements

The research results on which this publication is based are part of the project “New Cost-Effective and Reliable Test Environments (CERTEV)” that is funded by the Federal Ministry for Economics Affairs and Climate Action (BMWK) on the basis of a decision by the German Bundestag. The statements and information in this contribution do not necessarily represent the opinion of the BMWK. Publishing fees supported by Funding Programme Open Access Publishing of Hamburg University of Technology (TUHH)

Data availability

Data will be made available on request.

References

[1] F.R. Jones, J.P. Foreman, The response of aerospace composites to temperature and humidity, in: Polymer Composites in the Aerospace Industry, Elsevier, 2020, pp. 253–287.
[2] A. Redmann, M.C. Montoya-Ospina, R. Karl, N. Rudolph, T.A. Osswald, High-force dynamic mechanical analysis of composite sandwich panels for aerospace structures, Compos. Part C: Open Access 5 (2021) 100136.
[3] G.-C. Yu, L.-J. Feng, L.-Z. Wu, Thermal and mechanical properties of a multifunctional composite square honeycomb sandwich structure, Mater. Des. 102 (2016) 238–246.
[4] D. Göge, M. Böswald, U. Füllekrug, P. Lubrina, Ground vibration testing of large aircraft - state-of-the-art and future perspectives, in: IMAC-XXV; a Conference & Exposition on Structural Dynamics, 2007.
[5] L. Schwan, P. Hüttich, M. Wegner, D. Krause, Procedure for the transferability of application-specific boundary conditions for the testing of components and products, in: DS 111: Proceedings of the 32nd Symposium Design for X, The Design Society, 2021.
[6] P. Hüttich, D. Krause, Holistic approach to vibration characterization of large structural components in thermal environment, in: Proceedings of the ISMA2024, KU Leuven, Departement Werktuigkunde, LMSD (Mecha(tro)nic System Dynamics), Heverlee, 2024.
[7] P. Hüttich, S. Panek, D. Krause, Combined environments - challenges and potentials in the realistic component testing, in: DS 119: Proceedings of the 33rd Symposium Design for X, DFX2022, The Design Society, 2022, p. 10.
[8] M. Mobarakian, M. Safarabadi, M. Farahani, Developing a thermomechanical and thermochemical model for investigating the cooling rate effects on the distortion of unsymmetrical viscoelastic polymeric composite laminates, Polym. Test. 87 (2020) 106503.
[9] R. Sum, Influence of environmental factors on the component/equipment reliability, Indian J. Eng. Mater. Sci. (Vol. 5) (1998) 121–123.
[10] I. RTCA, RTCA/DO160G – environmental conditions and test procedures for airborne equipment, 2010.
[11] D. of Defense of the United States of America, MIL-std-810h - environmental engineering considerations and laboratory tests, 2019.
[12] X. Zu, H. Wu, H. Lv, Y. Zheng, H. Li, An amplitude- and temperature-dependent vibration model of fiber-reinforced composite thin plates in a thermal environment, Mater. (Basel, Switzerland) 13 (7) (2020).
[13] Z.Q. Wu, H.B. Li, W. Zhang, H. Cheng, F.J. KONG, B.R. Liu, Experimental investigation on dynamic response of aircraft panels excited by high-intensity acoustic loads in thermal environment, J. Physics: Conf. Ser. Vol. 744 (2016) 012092.
[14] M. Srivatsava, P.R. Sreekanth, Experimental characterization of dynamic mechanical properties of hybrid carbon-Kevlar reinforced composite with sandwich configuration, Mater. Today: Proc. 27 (2020) 931–935.
[15] C. Hernandez, A. Maranon, I.A. Ashcroft, J.P. Casas-Rodriguez, Inverse methods for the mechanical characterization of materials at high strain rates, EPJ Web Conf. 26 (2012) 04022.
[16] D. Lecompte, A. Smits, H. Sol, J. Vantomme, D. van Hemelrijck, Mixed numerical–experimental technique for orthotropic parameter identification using biaxial tensile tests on cruciform specimens, Int. J. Solids Struct. 44 (5) (2007) 1643–1656.
[17] M. Maeder, S. Chandra, S. Marburg, Identification of temperature dependent material properties in composite plates utilizing experimental vibration data, in: H. Altenbach, M. Beitelschmidt, M. Kästner, K. Naumenko, T. Wallmersperger (Eds.), Material Modeling and Structural Mechanics, in: Advanced Structured Materials, vol. 161, Springer International Publishing, Cham, 2022, pp. 115–134.
[18] Z. Ren, N. Atalla, S. Ghinet, Optimization based identification of the dynamic properties of linearly viscoelastic materials using vibrating beam technique, J. Vib. Acoust. 133 (4) (2011).
[19] K. Sepahvand, S. Marburg, Identification of composite uncertain material parameters from experimental modal data, Probabilistic Eng. Mech. 37 (2014) 148–153.
[20] K.S. Reddy, S. Somasundharam, An inverse method for simultaneous estimation of thermal properties of orthotropic materials using Gaussian process regression, J. Physics: Conf. Ser. 745 (2016) 032090.
[21] Y. Bai, K. Yu, R. Zhao, H. Zhou, Impact series Shaker excitation approach for structural modal testing in thermal environments, Exp. Tech. 42 (4) (2018) 429–438.
[22] Y. Bai, K. Yu, J. Zhao, R. Zhao, Experimental and simulation investigation of temperature effects on modal characteristics of composite honeycomb structure, Compos. Struct. 201 (2018) 816–827.
[23] S. Chandra, M. Maeder, J. Bienert, H. Beinersdorf, W. Jiang, V.A. Matsagar, S. Marburg, Identification of temperature-dependent elastic and damping parameters of carbon–epoxy composite plates based on experimental modal data, Mech. Syst. Signal Process. 187 (2023) 109945.
[24] R. Zhao, K. Yu, G.M. Hulbert, Y. Wu, X. Li, Piecewise shear deformation theory and finite element formulation for vibration analysis of laminated composite and sandwich plates in thermal environments, Compos. Struct. 160 (2017) 1060–1083.
[25] P. Jeyaraj, N. Ganesan, C. Padmanabhan, Vibration and acoustic response of a composite plate with inherent material damping in a thermal environment, J. Sound Vib. 320 (1–2) (2009) 322–338.
[26] M. Du, Q. Geng, Y.-m. Li, Vibrational and acoustic responses of a laminated plate with temperature gradient along the thickness, Compos. Struct. 157 (2016) 483–493.
[27] L. Li, Y. Hu, W. Deng, L. Lü, Z. Ding, Dynamics of structural systems with various frequency-dependent damping models, Front. Mech. Eng. 10 (1) (2015) 48–63.
[28] J. Han, K. Yu, X. Li, R. Zhao, Modal density and mode counts of sandwich panels in thermal environments, Compos. Struct. 153 (2016) 69–80.
[29] X. Li, K. Yu, R. Zhao, Vibro-acoustic response of a clamped rectangular sandwich panel in thermal environment, Appl. Acoust. 132 (2018) 82–96.
[30] A. Garg, H.D. Chalak, A review on analysis of laminated composite and sandwich structures under hygrothermal conditions, Thin-Walled Struct. 142 (2019) 205–226.
[31] M. Mobarakian, M. Safarabadi, M. Farahani, Investigating the effects of cooling rate on distortion of asymmetric composite laminates, Compos. Struct. 236 (2020) 111875.
[32] K. McConnell, Vibration Testing: Theory and Practice, John Wiley & Sons, New York, USA, 1995.
[33] A. Brandt, Noise and Vibration Analysis: Signal Analysis and Experimental Procedures, John Wiley and Sons Ltd, Chichester, UK, 2011.
[34] G.F. Lang, Electrodynamic shaker fundamentals, Sound Vib. Issue (1997) 1–8.
[35] G.F. Lang, D. Snyder, Understanding the physics of electrodynamic shaker performance, Dyn. Test. Ref. Issue (35) (2001) 24–35.
[36] E. Heyden, A. Lindenmann, S. Matthiesen, D. Krause, Approach for calibrated measurement of the frequency response for characterization of compliant interface elements on vibration test benches, Appl. Sci. 11 (20) (2021) 9604.
[37] Q. Geng, Y. Li, Solutions of dynamic and acoustic responses of a clamped rectangular plate in thermal environments, J. Vib. Control (2014).
[38] P. Hüttich, D. Krause, Frequency response fuctions of variant GFRP sandwich panel in thermal environment, 2024, http://dx.doi.org/10.15480/882.13619.